

Fermi National Accelerator Laboratory

FERMILAB-CONF-90/104-T

May 1990

THREE-FAMILY TOP QUARK MASS SPECTRUM*

Carl H. ALBRIGHT

Department of Physics, Northern Illinois University, DeKalb, Illinois 60115†

and

Fermi National Accelerator Laboratory, P.O. Box 500, Batavia, Illinois 60510‡

Abstract

We expand upon our previous Monte-Carlo-type study of 3-family mass matrices which lead to the experimentally-determined KM matrix and satisfy the constraints imposed by $B_d - \bar{B}_d$ mixing, $|V_{ub}/V_{cb}|$, B_K and CP violation. Scatter distributions in $|V_{ub}V_{cb}|$, ϵ'/ϵ and x_s vs. m_t are presented for the standard minimal Higgs structure as well as top quark mass histograms for the minimal and 2-doublet Higgs models. A top quark mass in the range of 100 - 200 GeV is strongly favored with all the constraints imposed, but if the lower bound on the CP-violating J -value is completely relaxed, a secondary probability peaking occurs in the mass histograms which lies above 220 GeV in the minimal Higgs model.

*Submitted to the 25th International Conference on High Energy Physics, Singapore, 1990

†Permanent address

‡BITNET Address: ALBRIGHT@FNAL



Although the top quark still remains an elusive experimental object with its lower mass bound now having been raised to 89 GeV by the CDF group at Fermilab,¹ theoretical extractions of its mass based on more detailed electroweak mixing data are becoming more refined. On the one hand, more accurate knowledge of the Z and W boson masses, decay widths and $\sin^2\theta_W$ enable one to compute the electroweak corrections to these quantities and thereby extract the top quark mass under the assumption that all other contributions are well understood. A top quark mass in the range 100 - 200 GeV has emerged in several recent analyses² of this type, with values of 130 and 170 GeV being singled out, for example.

On the other hand, more accurate information on the KM mixing matrix for charged current weak interactions, including $B-\bar{B}$ mixing³ and the $b \rightarrow u$ transition^{3,4} have enabled one to test rather severely the predictions for certain mass matrix models, where the top quark mass is adjusted to give a best fit to the mixing data. The simple 3-family model introduced thirteen years ago by Fritzsch⁵ based on hierarchical chiral symmetry breaking has been especially well studied and has survived more and more stringent comparisons with data. In the time since its introduction, however, its top quark mass prediction has climbed steadily from 12 GeV to 90 - 100 GeV. In fact, detailed studies⁶ by the present author and several others have indicated that this is the maximum allowed limit in this model, if the constraint coming from $B-\bar{B}$ mixing is imposed on top of the restrictions from the individual KM mixing matrix elements themselves. Since the experimental lower limit has reached 89 GeV as indicated above, this model is on the verge of being ruled out.

In light of this development, the author recently investigated⁷ the general set of 3-family Hermitian mass matrices of the form

$$\mathbf{M}^U = \begin{pmatrix} E_1 & A & D \\ A & E_2 & B \\ D^* & B & C \end{pmatrix}, \quad \mathbf{M}^D = \begin{pmatrix} E'_1 & A' & D' \\ A'^* & E'_2 & B' \\ D'^* & B'^* & C' \end{pmatrix} \quad (1)$$

with 16 parameters, where the Fritzsch model with just 8 parameters is obtained if one sets $E_1 = E_2 = D = E'_1 = E'_2 = D' = 0$. The starting point of this work was based on a previous analysis of hierarchical chiral symmetry breaking by Lindner and the author.⁸ Through study first of the rank 2 matrices, we have observed that the upper bound on the top quark mass of ~ 100 GeV in the Fritzsch model can be removed by allowing E_2 , and much more importantly, E'_2 to differ from zero in the ranges⁷

$$0 \leq E_2 \lesssim 3m_c, \quad -m_s \leq E'_2 \leq 0 \quad (2)$$

To keep tractable our search for mass matrix solutions satisfying the constraints to be enumerated below, we have considered the full rank 3 case for M^D with the hierarchy

$$0 = E'_1 \lesssim |A'|, |D'|, |E'_2| \ll |B'| \ll C' \quad (3)$$

and the rank 2 case for M^U with a similar ordering but taking $E_1 = E_2 = A = 0$. (A non-zero D plays an important role in controlling the size of $|V_{ub}/V_{cb}|$.) A careful but incomplete study of the extension to the rank 3 case for M^U indicated that the space of solutions was not noticeably enlarged. With the standard Higgs structure, the most probable values for the top quark mass were found to be 130 GeV and 160 GeV with the CP phase δ in the 2nd and 1st quadrant, respectively.

The results and allowed range for the top quark mass depend critically on the Higgs structure associated with the mass matrix model. Here we extend our analysis of the standard Higgs results and also present results for the two-doublet Higgs case. Unlike the radiative correction calculations cited earlier,² which depend somewhat on the neutral Higgs mass appearing in the standard model, in the mass matrix approach it is the appearance of the charged Higgs scalar and ratio of two vacuum expectation values which determine the $B - \bar{B}$ mixing and ϵ_K through the box diagram Higgs exchange graphs.⁹

We shall briefly summarize the acceptance criteria which were imposed to obtain

acceptable mass matrix solutions, since the procedure has been covered in our earlier paper⁷ and will be spelled out in greater detail in a future paper which examines the effects of the renormalization group equations for the Yukawa couplings. The 10 physical parameters, 6 quark masses, 3 KM mixing angles and CP phase, can be fit in general with suitable choices of the 16 matrix parameters in (1). We use the set of five quark masses defined at 1 GeV by Gasser and Leutwyler,¹⁰ taking the explicit values of $m_u = 3.5$ MeV, $m_d = 6.1$ MeV, $m_s = 120$ MeV, $m_c = 1.36$ GeV and $m_b = 5.3$ GeV which favor a higher top quark mass. A top quark mass at 1 GeV is then selected and the remaining parameters varied in the ranges indicated above in order to fit the 3-family KM mixing matrix determined by Schubert¹¹ to within one standard deviation accuracy:

$$(|V_{ij}|) = \begin{pmatrix} 0.9754 \pm 0.0004 & 0.2206 \pm 0.0018 & 0.0000 \rightarrow 0.0123 \\ 0.2203 \pm 0.0019 & 0.9743 \pm 0.0005 & 0.0460 \pm 0.0060 \\ 0.0015 \rightarrow 0.0205 & 0.0449 \pm 0.0062 & 0.9989 \pm 0.0003 \end{pmatrix} \quad (4)$$

Here $V = UU^\dagger$, where U and U' are unitary matrices which diagonalize M^U and M^D , respectively. For convenience, we use the projection operator technique of Jarlskog¹² to compute exactly the absolute squares of the KM mixing matrix elements. The top quark mass is then evolved from 1 GeV to $m_t(m_t)$ and evaluated according to the standard physical mass definition including QCD corrections.¹³

Due to the uncertainties appearing in (4) above, it proves useful to invoke several other conditions which constrain various combinations of masses and KM mixing parameters.¹³ In particular, we use the $B_d - \bar{B}_d$ mixing parameter³ $x_d = 0.66 \pm 0.09$ to define the range

$$\begin{aligned} m_t^2 |V_{td}^* V_{tb}|^2 R &\simeq (1.8 \pm 0.3) \frac{(0.140)^2}{\bar{B}_B f_B^2} \\ &\simeq 1.3 - 2.3 \end{aligned} \quad (5)$$

where R represents a correction factor depending on the running top quark mass, and we assume that the ratio of $b \rightarrow u$ to $b \rightarrow c$ transitions⁴ constrains the KM mixing

ratio to

$$|V_{ub}/V_{cb}| \simeq 0.07 - 0.15 \quad (6)$$

Furthermore, we impose the constraint on the K decay bag parameter, which enters the box diagram calculation for the CP-violating ϵ_K parameter,

$$B_K \simeq 0.55 - 0.90 \quad (7)$$

obtained from studies of corrections to the $1/N$ expansion by Bardeen, Buras and Gérard.¹⁴

Finally, we require that the Jarlskog J -value¹⁵ which is a measure of CP violation expressed in terms of the cosines and sines of the now standard KM matrix

$$\begin{aligned} J &= \text{Im} (V_{us} V_{cb} V_{ub}^* V_{cs}^*) \\ &\simeq c_{12} c_{13}^2 c_{23} s_{12} s_{13} s_{23} \sin \delta \\ &\simeq \pm |V_{us}| |V_{cb}| |V_{ub}| |V_{cs}| \sin \delta \end{aligned} \quad (8a)$$

lie in the range

$$|J| \simeq (3.0 \pm 0.5) \times 10^{-5} \quad (8b)$$

as estimated from the decay rate for $B_d \rightarrow K^- \pi^+$ by Donoghue, Nakada, Paschos and Wyler.¹⁶ We have calculated the J -value from the commutator of the M^U and M^D mass matrices¹⁵ and used (8a) to determine $\sin \delta$. Because $\sin \theta_{13}$ appearing in the ub element of V_{KM} is very small and can take either sign, we have allowed J to assume both signs and the CP phase δ to lie in either the second or first quadrant.

Since the recent measurements¹⁷ of the direct CP-violation parameter, ϵ'/ϵ , by the NA31 group at CERN and the E731 group at FNAL

$$\epsilon'/\epsilon = \begin{cases} (33 \pm 11) \times 10^{-4} & (NA31) \\ (-5 \pm 15) \times 10^{-4} & (E731) \end{cases} \quad (9)$$

are in some disagreement, we shall not use them to impose restrictions on the mass matrices. They can, however, be compared with the predictions below.

We first discuss the results for the standard minimal Higgs structure. The distributions in the J -value, $m_t^2|V_{td}^*V_{tb}|^2R$, $|V_{ub}/V_{cb}|$ and B_K were presented in detail earlier in our previous paper,⁷ so we begin with some general comments here. The well-determined ϵ_K parameter is proportional to the product of the bag parameter B_K , the J -value and a leading term in m_t^2 . Thus as m_t increases, the product JB_K is required to decrease until B_K and J each reach their lower bounds imposed above in (7) and (8), at which point the top quark mass distribution reaches its upper limit. This occurs at higher m_t^{phys} for the CP phase δ in the first quadrant, because some cancellation occurs with $\cos \delta$ positive. The restriction on the $B - \bar{B}$ mixing combination in (5) has a similar effect, but it is somewhat weaker since the V_{td} element is allowed to become quite small as given in the Schubert extraction¹¹ of (4).

In Fig. 1 we present the solution scatter plots which are presently of most interest: $|V_{ub}/V_{cb}|$, ϵ'/ϵ and x_s vs. m_t for $\cos \delta$ negative and positive. Values in the range $0.07 \lesssim |V_{ub}/V_{cb}| \lesssim 0.11$ are much preferred. The value of ϵ'/ϵ was calculated for each solution with the recent tabulation of Buchalla, Buras and Harlander,¹⁸ which included contributions from both weak and electromagnetic penguins. As they and also Paschos, Schneider and Wu¹⁸ have pointed out, ϵ'/ϵ can become negative for a top quark mass around 230 GeV. Our scatter distributions favor a value around $(0.6 - 0.7) \times 10^{-3}$ as the most likely and in better agreement with the E731 result, corresponding to the range of 130 - 160 GeV for the top quark mass cited above. The x_s distribution for $B_s - \bar{B}_s$ mixing, scaled relative to x_d by $|V_{ts}/V_{td}|^2$, rises nearly linearly with m_t from 5 to over 10, with 7 - 8 most favored. This is understood when one realizes that the V_{td} element is forced downward for a higher top quark mass.

In Fig. 2(a) and (b) we show the top quark mass histograms for δ in the second and first quadrants. Since ref. 7 was prepared, we have made the following observation. The J -value constraint in (8b) is probably the most uncertain of those imposed. If

we relax the lower bound completely and accept the range

$$|J| < 0.4 \times 10^{-4} \quad (8c)$$

a higher top quark mass is allowed than before such that the correct value for ϵ_K is still obtained. For $\cos \delta < 0$, the new region is obvious in Fig. 2(c), but the probability for a top quark mass above 200 GeV is not substantially increased. Not so for $\cos \delta > 0$ in Fig. 2(d), as a secondary peak develops in the 250 GeV mass range, though the most probable value is little changed from 160 GeV. Additionally, we note that the phase δ is forced to deviate from its maximal CP-violating value of 90° in the new lower J and higher top quark mass ranges. This also can be appreciated, as the minimum J -value determined from (4), (6) and (8a) is given by

$$\begin{aligned} |J|_{min} &= 0.2188(0.9738)(0.040)^2(0.07)\sin \delta \\ &\simeq 0.24 \times 10^{-4} \sin \delta \end{aligned} \quad (10)$$

In Fig. 3(a-c) and (d-f) we show the J , B_K and δ distributions with the two constraints (8b) and (8c), respectively, for δ in the first quadrant. By comparing Fig. 3(a) and (d) for J , 3(b) and (e) for B_K , and 3(c) and (f) for δ , one sees pictorially the remarks made above. With extension to a higher top quark mass, the $|V_{ub}/V_{cb}|$ distribution is little changed as values in the range 0.07 - 0.11 are still greatly favored. The ϵ'/ϵ distribution continues the downward trend shown in Fig. 1(e) with a second clustering of points occurring between 0 and -0.5×10^{-3} , while the x_s distribution continues the upward trend shown in Fig. 1(f) with values as large as 20 now possible. Of course one can argue that it is more reasonable simply to lower the bound on J down to 0.20×10^{-4} . In this case the general effects are still present but not so pronounced, especially for $\cos \delta > 0$.

Finally we turn to the two-doublet Higgs model. For purposes of illustration the ratio of vacuum expectation values has been set equal to unity and a charged scalar

Higgs mass of 50 and 90 GeV selected. In this model it is assumed the top quark can decay into a bottom quark and charged Higgs scalar. The charged Higgs also contributes to the box diagrams⁹ for $B - \bar{B}$ mixing and ϵ_K . The net interference with the W exchange graphs is constructive, so the R factor in (5), and similarly in ϵ_K , is enhanced above unity.¹³ As a result, the product JB_K is forced to decrease more rapidly as m_t increases, with the result that the top quark mass limit is lower than in the standard Higgs model. We present the top quark mass histograms in Figs. 4 and 5 for the 50 and 90 GeV choices, respectively, with δ in the second and first quadrant and the constraint 8(b) imposed in (a) and (b), while the relaxed constraint 8(c) is imposed in (c) and (d). From the histograms in Fig. 4(a,b) and 5(a,b) one finds a relatively low top quark mass is favored in the range 90 - 120 GeV; however, if the lower bound on J in (8b) is relaxed to (8c), secondary peaks in the histograms develop in the 160 - 180 mass range, especially for δ in the first quadrant.

In conclusion, we see that a top quark mass in the 100 - 200 GeV range is much preferred, in agreement with the electroweak correction calculations of ref. 2, unless the lower bound on the J -value is substantially relaxed. In the latter case with standard minimal Higgs structure, the top quark mass develops a fair probability of appearing above 200 GeV. In this regard, we recall the dynamical symmetry-breaking prediction of 230 GeV preferred by Bardeen, Hill and Lindner¹⁹ which clearly requires the latter scenario. The Fritzsche model⁵ with its top quark mass confined to the 90 - 100 GeV range is clearly disfavored by the present lower experimental bound¹ of 89 GeV; however, it is interesting to note that the 3-family mass matrices scanned by this Monte Carlo type study all evolve from the Fritzsche model in the same or higher order. The hierarchical chiral symmetry-breaking scenario proposed by Fritzsche is not a bad lowest order approximation after all.

The author thanks the Theory Department of Fermilab for its kind hospitality during the course of this work. This research was supported in part by Grant No. PHY-8907806 from the National Science Foundation. Fermilab is operated by Universities Research Association, Inc. under contract with the United States Department of Energy.

References

- [1] G. P. Yeh, *Les Recontres de Physique de la Valle d'Aoste*, M. Greco Editor, Editions Frontieres, Gif-sur-Yvette 1990.
- [2] J. Ellis and G. L. Fogli, *B* 232 (1989) 139; P. Langacker, *Phys. Rev. Lett.* 63 (1989) 1920; V. Barger, J. L. Hewett and T. G. Rizzo, University of Wisconsin preprint MAD/PH/564; J. L. Rosner, University of Chicago preprint EFI 90-18; W. A. Bardeen and C. T. Hill, manuscript in preparation.
- [3] M. V. Danilov, in *Proceedings of the XIV International Symposium on Lepton and Photon Interactions*, Stanford, 1989; D. L. Kreinick, *ibid.*
- [4] R. Fulton et al., *Phys. Rev. Lett.* 64 (1990) 16.
- [5] H. Fritzsch, *Phys. Lett. B* 70 (1977) 436; *B* 73 (1978) 317; *B* 166 (1986) 423.
- [6] C. H. Albright, *Phys. Lett. B* 227 (1989) 171 and references therein.
- [7] C. H. Albright, *Phys. Lett. B*, to be published.
- [8] C. H. Albright and M. Lindner, *Z. Phys. C* 44 (1989) 673.
- [9] G. G. Athanasiu and F. J. Gilman, *Phys. Lett. B* 153 (1985) 1393; G. G. Athanasiu, P. J. Franzini and F. J. Gilman, *Phys. Rev. D* 32 (1985) 3010; S. L. Glashow and E. E. Jenkins, *Phys. Lett. B* 196 (1987) 233.

- [10] J. Gasser and H. Leutwyler, Phys. Rep. 87 (1982) 77.
- [11] K. R. Schubert, in Proceedings of the 1987 EPS Conference, Uppsala, 1987.
- [12] C. Jarlskog, Phys. Rev. D 35 (1987) 1685; D 36 (1987) 2138; C. Jarlskog and A. Kleppe, Nucl. Phys. B 286 (1987) 245.
- [13] C. H. Albright, C. Jarlskog and B.-Å. Lindholm, Phys. Lett. B 199 (1987) 553; Phys. Rev. D 38 (1988) 872.
- [14] W. A. Bardeen, A. J. Buras and J.-M. Gérard, Phys. Lett. B 211 (1988) 343.
- [15] C. Jarlskog, Phys. Rev. Lett. 55 (1985) 1039 and Zeit. Phys. C 29 (1985) 491.
- [16] J. F. Donoghue, T. Nakada, E. A. Paschos and D. Wyler, Phys. Lett. B 195 (1987) 285.
- [17] H. Burkhardt et al., Phys. Lett. B 206 (1988) 169; B. Winstein, in Proceedings of the XIV International Symposium on Lepton and Photon Interactions, Stanford, 1989.
- [18] G. Buchalla, A. J. Buras and M. K. Harlander, Max Planck Institute preprint MPI-PAE/PTh 63/89. See also the ϵ'/ϵ analysis of E. A. Paschos, T. Schneider and Y. L. Wu, Fermilab preprint FERMILAB-CONF-90/48-T.
- [19] W. A. Bardeen, C. T. Hill and M. Lindner, Phys. Rev. D 41 (1990) 1647.

Figure Captions

- Figure 1: Scatter plots of (a) $|V_{ub}/V_{cb}|$, (b) ϵ'/ϵ and (c) x_s vs. m_t for mass matrix solutions with standard Higgs structure which satisfy the criteria of (4) - (8b) with the CP phase δ in the second quadrant. Similar plots in (d), (e) and (f) apply for δ in the first quadrant.
- Figure 2: Histograms for the top quark mass with standard Higgs structure and the full set of constraints with δ in (a) the second and (b) the first quadrant. In (c) and (d) the constraint (8b) on J is relaxed to that in (8c).
- Figure 3: Comparison of the standard Higgs model scatter plots for J , B_K and δ vs. m_t with δ in the first quadrant and the full set of constraints in (a), (b) and (c) versus (d), (e) and (f) with the J -value constraint relaxed as in (8c).
- Figure 4: Top quark mass histograms in the two-doublet Higgs model with full constraints, equal vacuum expectation values, a 50 GeV charged Higgs scalar and δ in (a) the second and (b) first quadrant. In (c) and (d) the constraint in (8b) is replaced by (8c).
- Figure 5: The same histograms are exhibited as in Fig. 4 for a 90 GeV charged Higgs scalar.

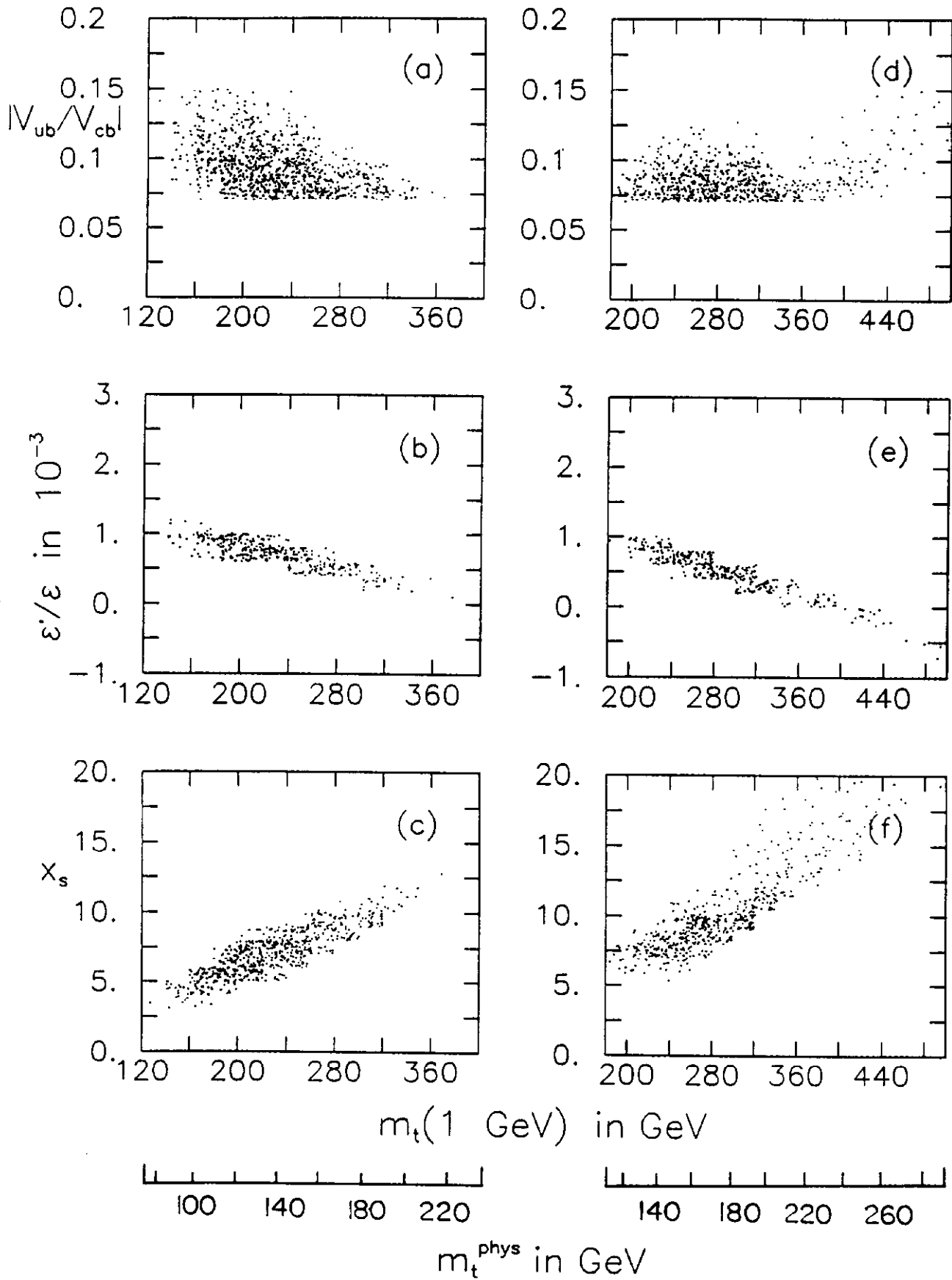


Fig. 1

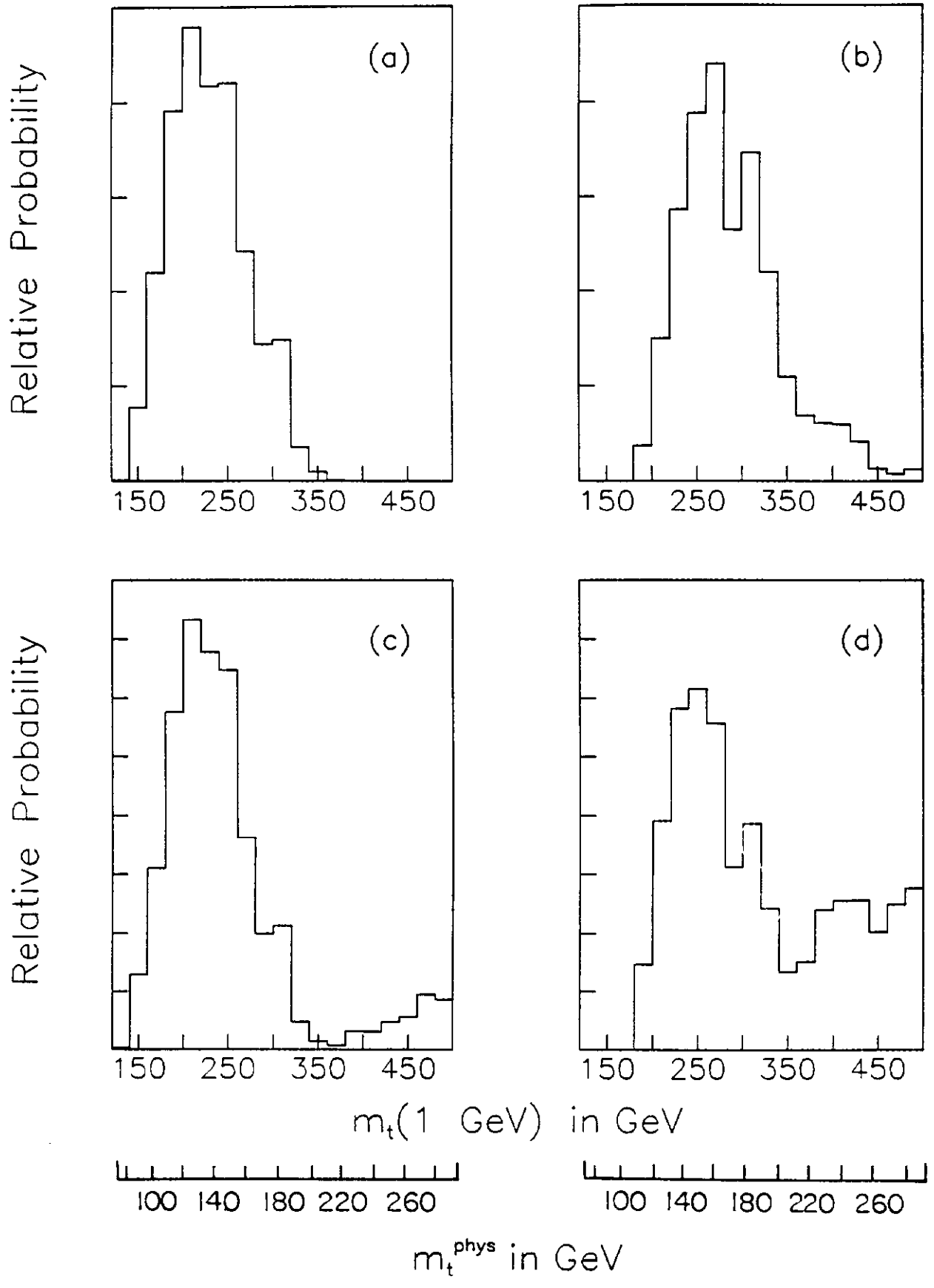


Fig. 2

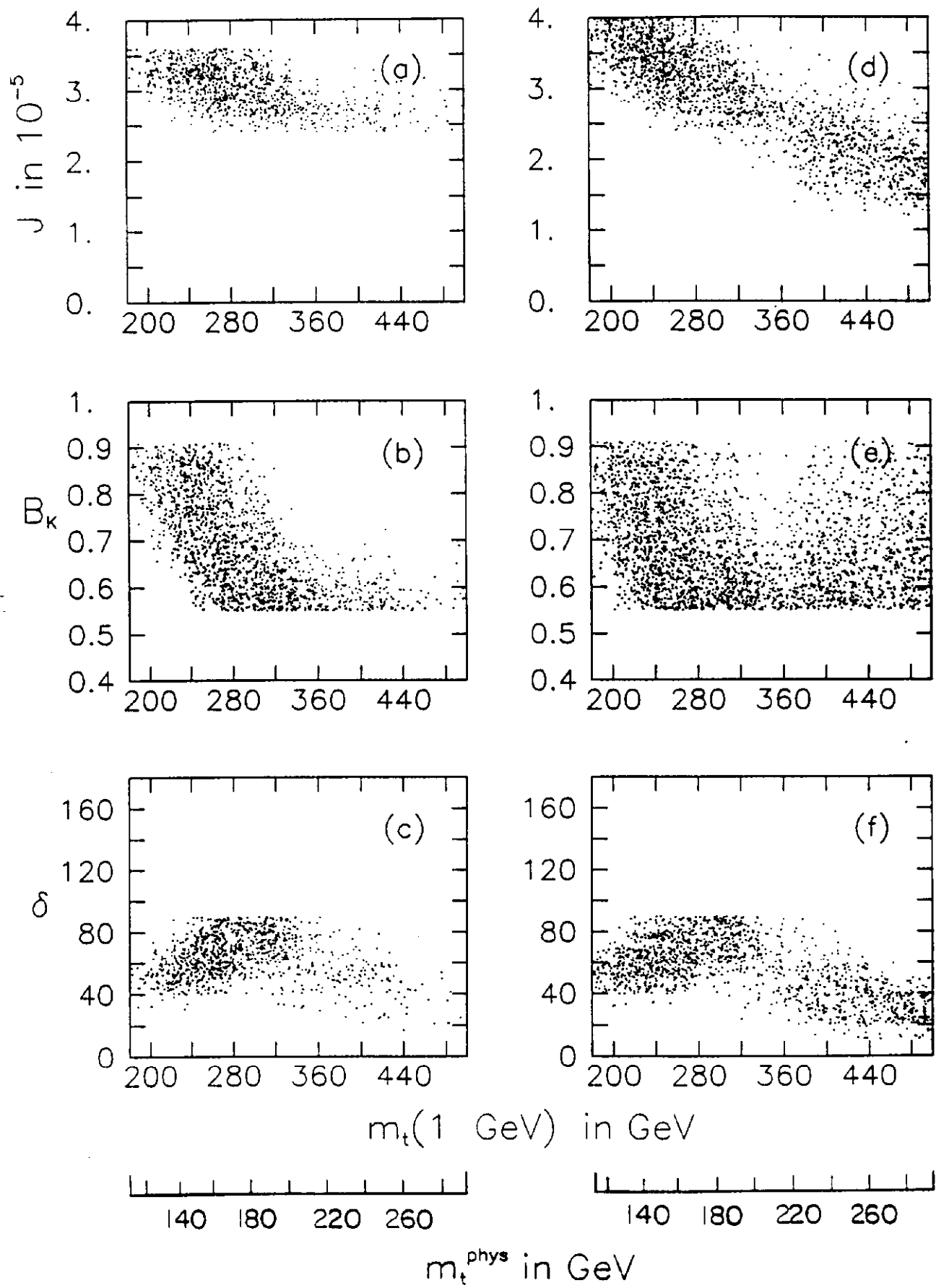


Fig. 3

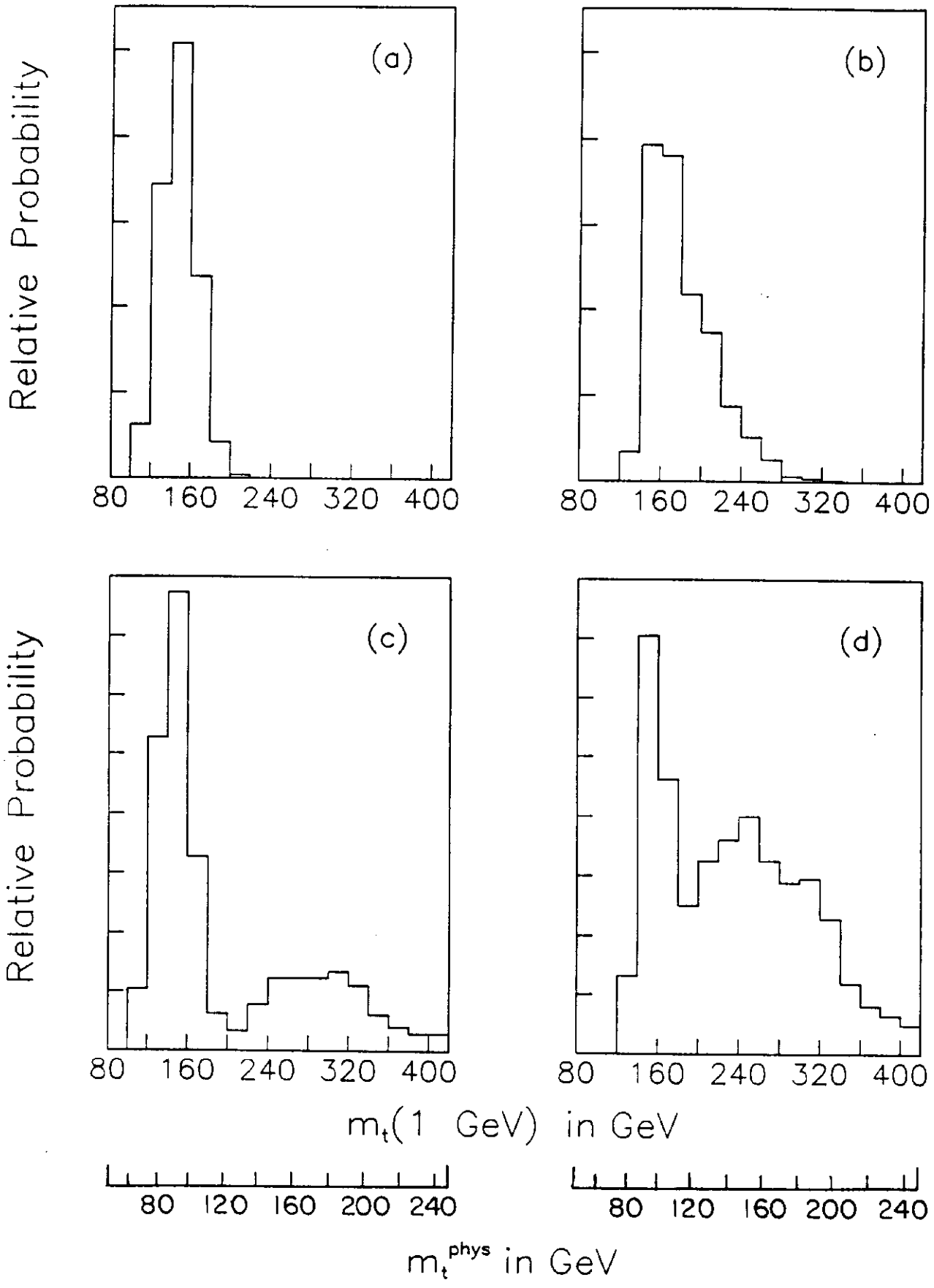


Fig. 4

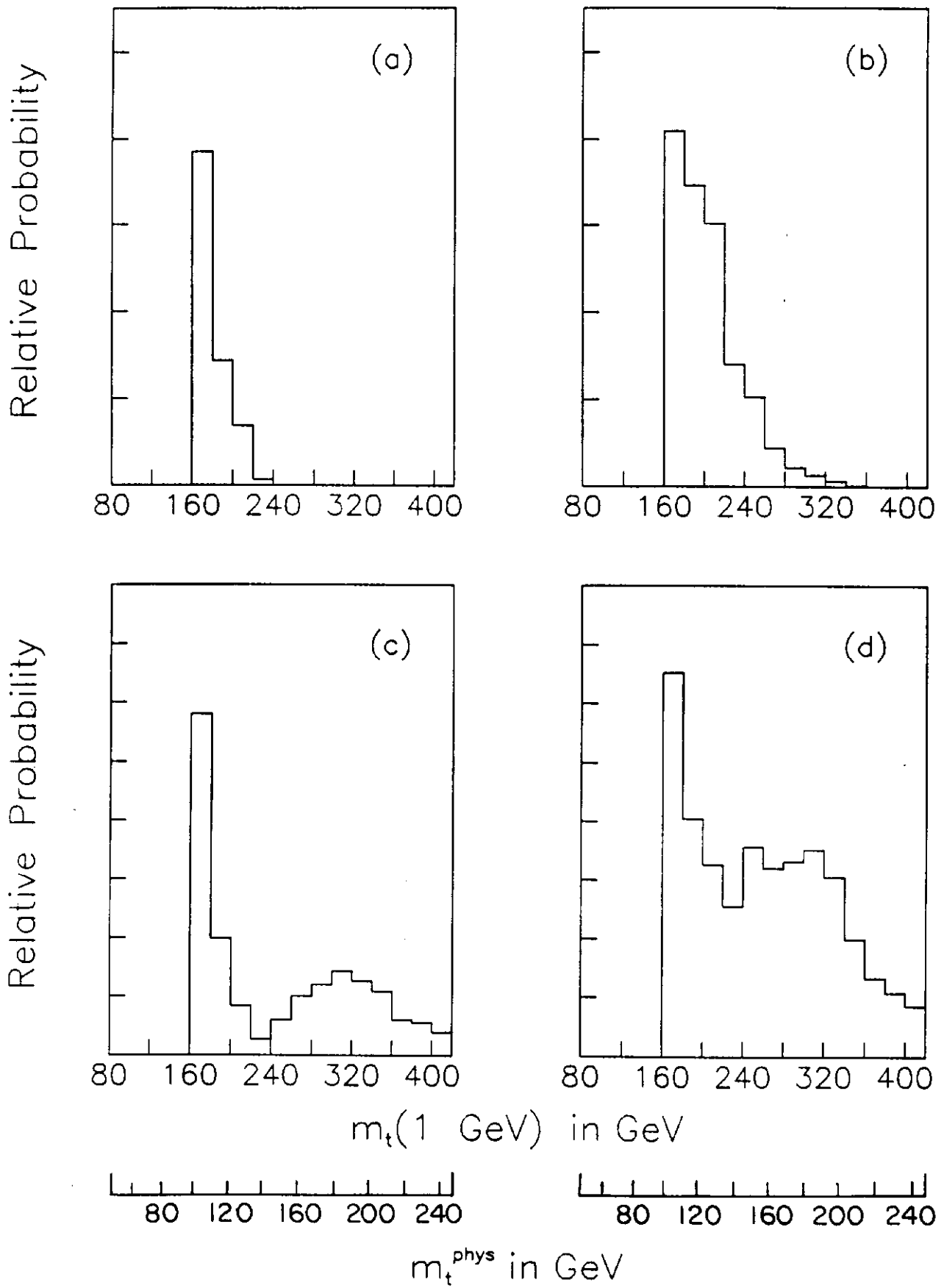


Fig. 5